JOURNAL OF MATERIALS SCIENCE **34** (1999) 1117–1127

The kinetics of isothermal β' precipitation in Al-Mg alloys

M. J. STARINK*, A.-M. ZAHRA
Centre de Thermodynamique et de Microcalorimétrie du CNRS, 13331 Marseille Cedex 3, France

Isothermal β' precipitation in Al-14 at % Mg and Al-16 at % Mg is studied by isothermal calorimetry, differential scanning calorimetry, and optical and transmission electron microscopy. The characteristic length of the β' precipitates varies strongly with ageing temperature, indicating that the definition of a state variable is not possible. As a consequence the commonly used equation:

$$\frac{d\alpha}{dt} = g(T)f(\alpha)$$

with $f(\alpha)$ a function depending only on the fraction transformed, and $g(T)$ a function of temperature, is not valid for this reaction. The isothermal calorimetry curves can be fitted over the entire range of transformation by a recently developed variant of the Johnson-Mehl-Avrami-Kolmogorov (JMAK) model. For $T < 160\,^{\circ}C$ and $T > 200\,^{\circ}C$ the reaction exponent n is larger than 2.5, indicating an autocatalytic precipitation process. The mechanisms for this autocatalytic process are discussed.

1. Introduction

Although different symbols for the zones and phases have been used, most work on the precipitation in Al-rich Al-Mg alloys [1–5] indicates the following precipitation sequence (symbols as used in [1]):

$$\text{sss}\alpha \rightarrow \text{GP zones} \rightarrow \beta'' \rightarrow \beta' \rightarrow \beta$$

where sssα is the supersaturated solid solution, GP zone (also indicated as δ'') stands for Guinier-Preston zone, β'' (other indications: ordered GP zone [6] or δ') is an $L1_2$ ordered phase with composition Al_3Mg [7] appearing as approximately spherical coherent precipitates, β' is a semicoherent hexagonal intermediate phase (approximate composition Al_3Mg_2) with lattice parameters $a = 1.002$ nm and $c = 1.636$ nm [4, 8], it is the main hardening precipitate [9], and β is the equilibrium phase (approximate composition Al_3Mg_2) having a complex FCC structure with $a = 2.824$ nm [4].

When solid solutions with up to 17 at % Mg are aged at temperatures in excess of about 90 °C, no $L1_2$ ordered structures or zones form. In solid-quenched and liquid-quenched Al-Mg aged between about 110 and 250 °C the β' phase forms first [4, 10]. Several explanations for the nucleation mechanisms of β' have appeared in the literature. From a transmission electron microscopy (TEM) study on precipitation in Al-8.8 at % Mg and Al-9.9 at % Mg alloys Bouchear *et al.* [5] concluded that β' nucleates on dislocation loops which are abundantly present in Al-Mg alloys, and this interpretation is in agreement with early work by Embury and Nicholson [11]. Conversely, from a TEM study on precipitation in an Al-8.7 at % Mg alloy Itoh *et al.* [12] concluded that dislocation loops played no role in the nucleation of β', and this latter interpretation is in agreement with early TEM work by Eikum and Thomas [13]. In the grains the β phase only appears in the later stages of ageing when the Mg depletion of the matrix is nearly completed [4, 10], and TEM in combination with differential scanning calorimetry (DSC) experiments [14] have shown that β phase formation mainly occurs through the transformation of β' precipitates. Further, the equilibrium β phase is observed on grain boundaries, even in solution treated and quenched alloys.

Although precipitation in binary Al-Mg alloys has been studied by many researchers, several questions relating to the nucleation of β', the kinetics of β' formation and the influence of vacancies and other defects on β' formation have remained unanswered. For this reason we performed isothermal and some non-isothermal ageing experiments on Al-Mg alloys and studied samples using optical microscopy, TEM, DSC and isothermal calorimetry in the temperature range 130–260 °C.

* *Current address*: Department of Engineering Materials, University of Southampton, Southampton S017 1BJ, UK.

TABLE I Compositions of the alloys

Alloy	Mg (at %)	Mg (wt %)	Al
Al-14Mg	13.7	12.5	Balance
Al-16Mg	15.8	14.5	Balance

2. Experimental

2.1. Alloys

High purity alloys with nominal compositions Al-14Mg and Al-16Mg were produced by conventional casting and subsequent rolling at Centre de Recherches de Voreppe (Aluminium Pechiney). The chemical analysis of the alloys is presented in Table I. Typical total impurity content is about 0.03 mass % (mainly Si). The grain size is large: about 0.2 mm.

2.2. Calorimetry

For the calorimetric experiments batches of 20 disk shaped samples of 1 mm thickness were prepared from each alloy. Multiple experiments were performed on a single batch and when the mass increase of a batch due to oxidation exceeded 0.1% that batch was discarded and a new batch was used. A differential Tian-Calvet microcalorimeter with two furnaces fixed above it combined with an automatic introduction system was employed. Generally the sample batch was solution treated at 440 °C for 2 h in the top furnace and subsequently lowered into the lower furnace. The set temperature of this furnace (20 °C below the calorimeter temperature) and the hold time of the sample (about 150 s) were chosen such that the sample reached a temperature close to the calorimeter temperature. We will term this cooling procedure furnace cooling. Apart from these furnace-cooled specimens also ice-water quenched (IWQ) specimens and samples cooled in air (for 3 min) were studied. As water quenching caused many calorimetry specimens to crack, only a single calorimetry experiment on a batch of IWQ specimens was performed.

The calorimeter used for the isothermal heat flow experiments possesses an excellent base line stability coupled with a high sensitivity (down to a microwatt). Ageing temperatures between 130 and 260 °C at intervals of about 10 °C, and times up to 7 days were employed. Due to the insertion of the specimen the heat flow measurement in the calorimeter is initially disturbed, and the heat flow due to the transformation in the sample can not be measured during the first 20 min. Generally 3 experiments per temperature were performed; the repeatability of the heat flow and of the time at maximum exothermic heat flow are both typically about 99%. The baseline of the microcalorimeter was determined at each temperature by performing experiments with pure Al.

2.3. Differential scanning calorimetry

For DSC experiments disks of 6 mm diameter and height 1 mm (average mass about 70 mg) were machined from homogenised ingots. The alloys were heat treated according to the above described procedures. Artificial ageing treatments were concluded by cooling in air. DSC experiments were performed using a Perkin-Elmer 1020 series DSC7. Detailed descriptions of the DSC apparatus and calibration procedures have been presented elsewhere [15, 16]. DSC runs were performed at 20 °C/min between 0 and 460 °C.

2.4. TEM and optical microscopy

For TEM experiments samples were heat treated in the calorimeter according to the above described procedures and were subsequently stored in liquid nitrogen. The specimens were ground to about 100 μm and electropolished in a 3 : 1 mixture of methanol and HNO_3 at −20 °C. The foils were examined in a Philips EM 400 T microscope operated at 100 kV, a JEOL JEM 2000 microscope operated at 200 kV and a JEOL JEM 2010 F microscope operated at 200 kV. On average 3 samples per heat treatment were studied.

For optical microscopy polished samples were etched in Keller and Wilcox' reagent (∼1% HF, 2.5% HNO_3 and 2% HCl in water).

3. Nucleation and growth reactions at constant temperature

In interpreting the data on the precipitation in Al-Mg we will make use of the general theory of reaction kinetics. In this section we will give a short overview of recent developments in this area which are of importance for the present work.

The transformation is described using an analysis recently developed by the present authors [14, 16, 17]. Similar to the Johnson-Mehl-Avrami-Kolmogorov (JMAK) kinetics [18–22] the present model uses the so-called 'extended volume' concept (see also [23]). In the 'extended volume' the individual nuclei grow without any limitation of space. In applying this concept first the volume, V_p, of the transformed region at time t which nucleated at an earlier time z will be calculated. For diffusion controlled precipitation reactions, we will define the transformed volume to be the volume of an imaginary fully depleted area around a precipitate (with the rest of the matrix undepleted) needed to give a precipitate size equal to the real case with a diffusion zone. In general it holds:

$$V_p = C[G(t - z)]^m \tag{1}$$

where G is the (average) growth rate, C is a constant which is related to the initial supersaturation, the dimensionality of the growth and the mode of transformation whilst the m is a constant related to the dimensionality of the growth and the mode of transformation, i.e. diffusion controlled growth or growth in which each part of the interface has a constant velocity (so-called linear growth). An overview of the values of the growth exponent, m, that occur for different types of reactions has been given in [19, 24]. Equation 1 is valid for equiaxed particles for which the growth rate is constant in all directions. It is also valid for elongated particles, provided that the ratios of the growth rates in the different

directions remain constant, i.e. provided that the particle retains the same shape. In this case G is an average of the growth rate over all directions.

Next the contribution of nucleation is considered. The amount of nuclei formed in volume V_0 during a time interval dz is given by $I(z)V_0\,\mathrm{d}z$, where $I(z)$ is the nucleation rate per unit volume at time z. Then the contribution of the particles which nucleated during the time interval $(z, z+\mathrm{d}z)$ to the amount of transformed volume in the 'extended volume' at time t, $V_{\mathrm{ext}}(t)$, is obtained from Equation 1:

$$\mathrm{d}V_{\mathrm{ext}} = CI(z)V_0[G(t-z)]^m\,\mathrm{d}z \tag{2}$$

Integrating and introducing $\alpha_{\mathrm{ext}} = V_{\mathrm{ext}}/V_0$ yields:

$$\alpha_{\mathrm{ext}} = \int_0^t CI(z)[G(t-z)]^m\,\mathrm{d}z \tag{3}$$

Note that $\lim_{t\to\infty}\alpha_{\mathrm{ext}} = \infty$.

For several expressions of the nucleation rate $I(z)$ analytical expressions for Equation 3 can be derived. If the nucleation rate is constant during the entire transformation one obtains:

$$\alpha_{\mathrm{ext}}(I = \text{constant}) = A_2 I G^m t^{m+1} \tag{4}$$

where A_2 is a constant. When all nuclei are formed whilst α is still negligible, i.e. when the nucleation rate is zero during practically the entire transformation, α_{ext} is given by:

$$\alpha_{\mathrm{ext}}(I = 0) = A_3 G^m t^m \tag{5}$$

where A_3 is a constant. This case arises for the limit of $I(z)$ decreasing infinitely fast, and it can for instance arise when the number of nucleation sites is limited and all sites are used for nucleation very early on in the transformation. This case has been referred to as 'site saturation', and this term is adopted in this work. Hence for both cases (Equations 4 and 5) one obtains:

$$\alpha_{\mathrm{ext}} = [k(T)t]^n \tag{6}$$

with $k(T)$ a temperature dependent factor determined by A_2, G and I, or (for the site saturation case) A_3 and G. Also for $I(z) \sim t^a$, with a an integer larger than unity, Equation 3 results in an expression like Equation 6 (with in this case $n = m + 1 + a$). However, during an isothermal experiment the nucleation rate can only in a limited number of special cases be expected to increase with time. One such case is autocatalytic nucleation: the presence of nuclei enhances the probability of formation of other nuclei.

To obtain a general kinetic equation, the effect of impingement should next be included. Here we will simply consider that two kinetic equations which have been successful in describing transformation kinetics, the Austin-Rickett (AR) equation [24, 25] and the JMAK equation [18, 24], can both be derived from (see also [25]:

$$\frac{\mathrm{d}\alpha}{\mathrm{d}\alpha_{\mathrm{ext}}} = (1-\alpha)^{\lambda_i} \tag{7}$$

where λ_i will be termed the impingement factor. (Note that for the case of no impingement, i.e. $\alpha_{\mathrm{ext}} = \alpha$, $\lambda_i = 0$.) The JMAK equation is obtained for $\lambda_i = 1$, whilst the AR equation [16, 24] is obtained for $\lambda_i = 2$. The general solution of Equation 7 for $\lambda_i \neq 1$ is:

$$\alpha = 1 - \left(\frac{\alpha_{\mathrm{ext}}}{\eta_i} + 1\right)^{-\eta_i} \tag{8}$$

where $\eta_i = 1/(\lambda_i - 1)$. The JMAK equation is obtained for the case of $\lambda_i = 1$:

$$\alpha = 1 - \exp(-[k(T)t]^n) \tag{9}$$

Alternatively the JMAK equation is obtained from Equation 8 for the limit of $\eta_i \to \infty$. Thus Equation 8 incorporates both the AR equation and the JMAK equation, and by fitting Equation 8 to experimental transformation data the obtained parameters n and η_i will give information about the mechanism of the reaction. (Further also the case of no impingement, $\lambda_i = 0$, can be described by Equation 8.) In Section 4 this analysis method will be applied to calorimetry curves obtained for Al-Mg.

4. Results

4.1. TEM and optical microscopy

The precipitation of β' on ageing at 130, 190 and 252 °C was studied using TEM. Consistent with its published limits of stability [1, 26] no superspots due to an $L1_2$ ordered phase were noted in the selected area diffraction (SAD) patterns.

The development of the microstructure during ageing at 190 °C is presented in Fig. 1. After 1 h the sample contains some precipitates, whilst a zig-zag type contrast evidences dislocations with a direction inclined to the foil surface (Figs 1a and b). These dislocations seem to be independent of the precipitates and are not observed for longer ageing times. The density of the precipitates increases with ageing time (see Fig. 1c), and for long ageing times (>17 h) the plate-shaped precipitates could be identified as β' phase by their characteristic SAD patterns in the Al [110] direction (see Fig. 2). For shorter ageing times no identifiable SAD patterns of the precipitates could be obtained, but it is assumed that all plate-shaped particles are β' phase. Tilting showed that in accordance with their habit planes three possible orientations of the β' plates within one grain exist. The defects observed after 1 h ageing (Fig. 1b) appear to be spatially unrelated to β' precipitates, i.e. β' nucleation appears to be independent of the defects. The defects were not observed after longer ageing times.

Hardly any equilibrium β phase was observed and only after 17 h at 190 °C significant amounts ($\sim$ a few percent of the β' volume) were present. This late

appearance of the equilibrium phase (at this stage about 84% of the total heat evolution is completed) is consistent with results obtained by Bernole [4]. Special attention was paid to check for β phase growing on the β' particles; only for a small minority of β this appeared to be the case. The latter observation is in agreement with TEM work by Bouchear *et al*. [5].

Optical microscopy on Al-16Mg samples aged at 190 and 250 °C after furnace cooling revealed that the distribution of precipitates in this alloy is essentially

(a)

(b)

Figure 1 Bright field TEM micrographs of samples aged at 190 °C for 1 h (a) and (b), and 17 h (c). All micrographs show β' precipitates (several micrometers in length), whilst a and especially b additionally show a zig-zag type contrast due to dislocations with a direction inclined to the foil surface. (*Continued*).

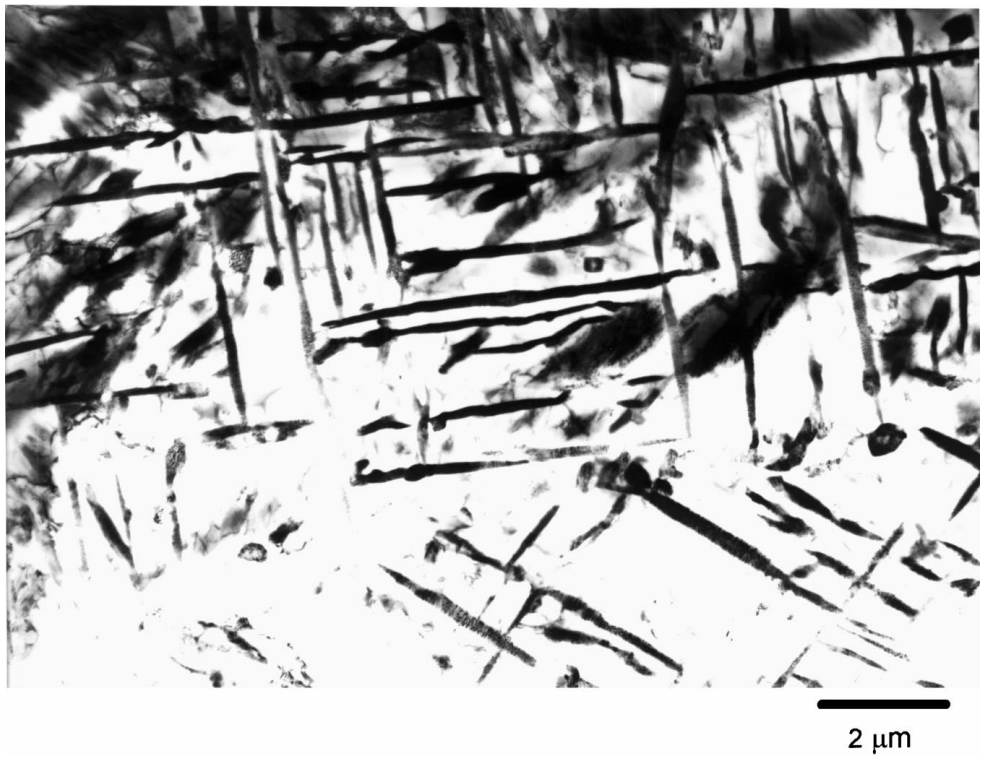

(c)

Figure 1 (*Continued*).

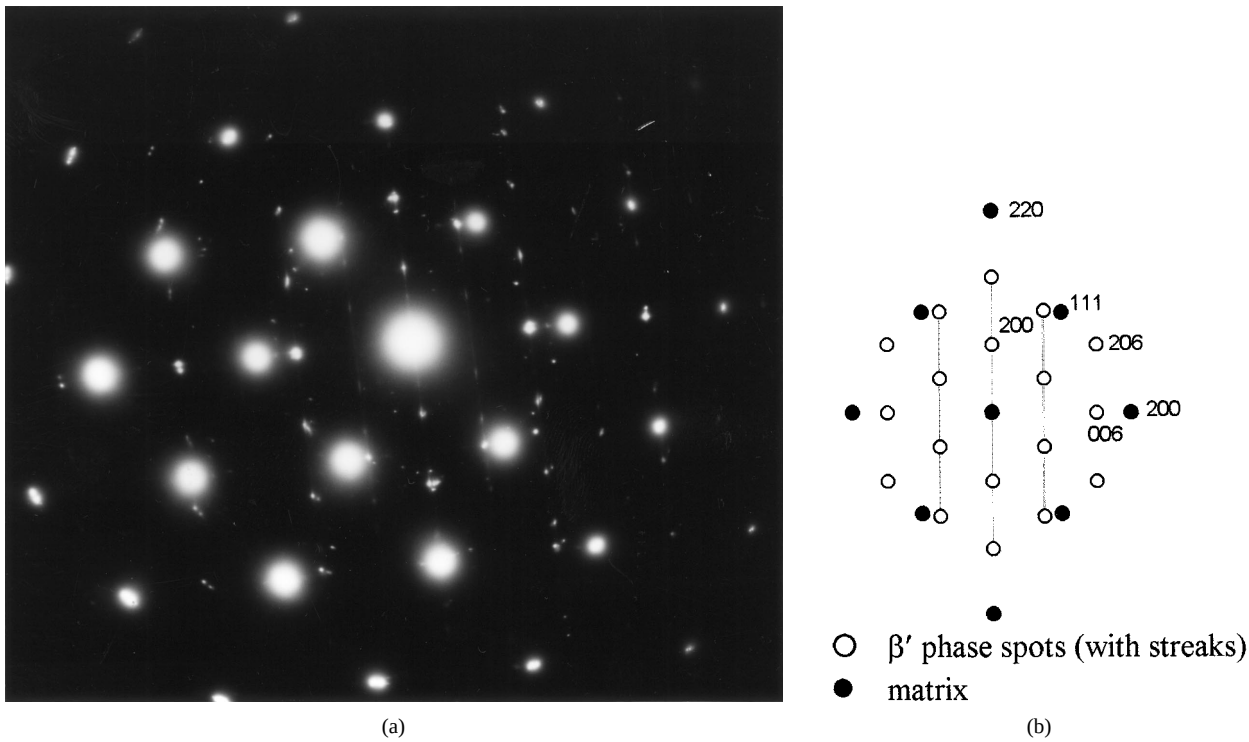

(a) (b)

Figure 2 SAD pattern of a β' particle (a), with the identification of the spots (b). $B = [110]$. Note that for the β' phase the 006 spots are the strongest ones.

homogeneous. Hamana *et al*. [27, 28] showed that in some Al-Mg based alloys β' precipitation can occur via the formation of precipitate clusters (sometimes in the shape of so-called rosettes). Unlike our alloys, those of Hamana *et al*. were of commercial purity and further contained significant amounts of Si, and hence it is possible that ternary alloying elements or impurities are the cause of the formation of precipitate clusters.

As the maximum dimensions of β' plates are always larger than the TEM foil thickness, it is not possible to draw definitive conclusions about the exact shape of the precipitates. It has, however, been suggested that

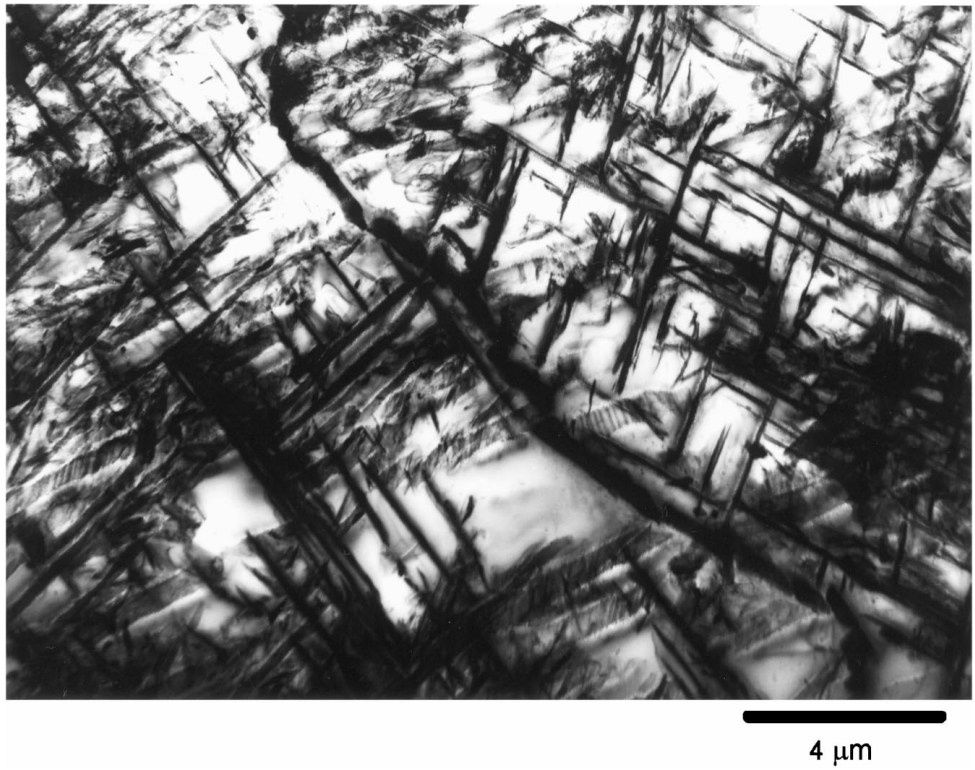

(a)

(b)

Figure 3 TEM microstructure of the Al-16Mg sample aged at 130 °C for 96 h (a) and for 1.7 h at 252 °C (b).

the β' plates have roughly the same dimensions in all directions parallel to its broad surface, i.e. they are approximately disc-shaped [4]. To study the growth of the β' plates their average lengths in all of the orientations appearing on the micrograph were measured and the orientation with the largest average length, l_{max}, was selected for further study. The l_{max} values obtained from different micrographs in randomly chosen foil orientations (about 5 for each ageing treatment) were averaged to obtain a characteristic length, l_{ch}, of the β' plates. From the method of calculating l_{ch} it is clear that l_{ch} is somewhat smaller than the maximum dimension of the β' plates, i.e. $l_{ch} = f l_{max}$, with $f < l$. However, if the β' plates are always approximately disc-shaped, f will

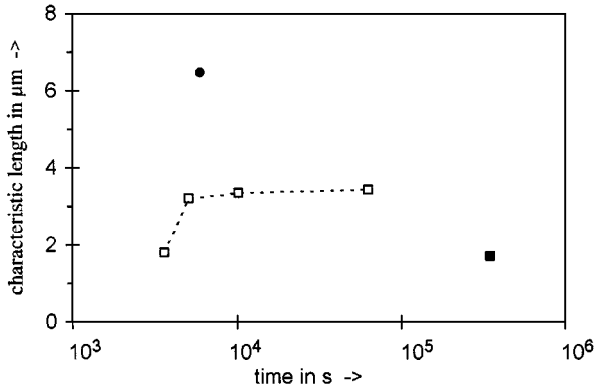

Figure 4 The characteristic lengths, l_{ch}, of the β' precipitates during ageing at 130 °C (■), 190 °C (□) and 252 °C (●).

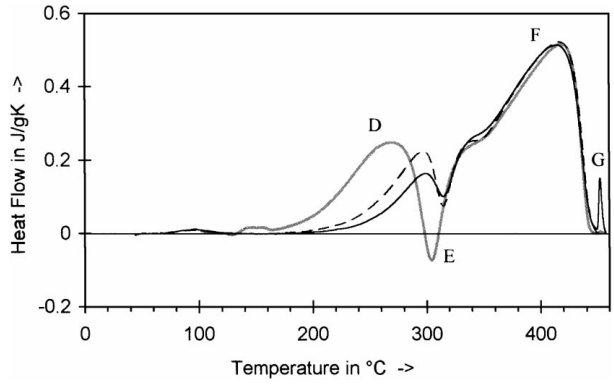

Figure 7 DSC curves of Al-16Mg samples aged for 6 days at 150 °C (grey line), 20 h at 190 °C (dotted line) and 5 h at 220 °C (solid line).

be a constant and l_{ch} is truly a characteristic dimension of the β' plates. The results of the determinations of l_{ch} are presented in Fig. 4.

Consistent with the large grain size very few grain boundaries were observed in TEM foils. Some of them contained continuous β phase precipitates.

4.2. Kinetic analysis of β' formation by calorimetry

Isothermal calorimetry was used to study β' formation in the Al-16Mg alloy during ageing at temperatures between 130 and 260 °C. Selected normalised heat evolution curves are presented in Fig. 5. For comparison isothermal calorimetry at 190 and 220 °C was also performed for the Al-14Mg alloy. In Fig. 6 the results for the two alloys are compared. As can be expected from the lower Mg content of the Al-14Mg alloy, the heat content of the exothermic effect in this alloy (-1130 ± 30 J/mol at 190 °C and -1080 J/mol at 220 °C) is lower as compared to the Al-16Mg alloy (-1660 J/mol at 190 °C and -1840 J/mol at 220 °C). If the type of precipitating phase does not change with temperature, a decrease of the exothermic heat content with ageing temperature, as observed for the Al-14Mg alloy, can be explained by an increase of solid solubility with temperature. Clearly, this explanation is not valid for the Al-16Mg alloy, and the increase of the evolved heat with temperature for this alloy has been explained in terms of a change in precipitation from mainly β' formation at low temperatures to precipitation resulting in a state with nearly exclusively β phase at higher temperatures (see [14]).

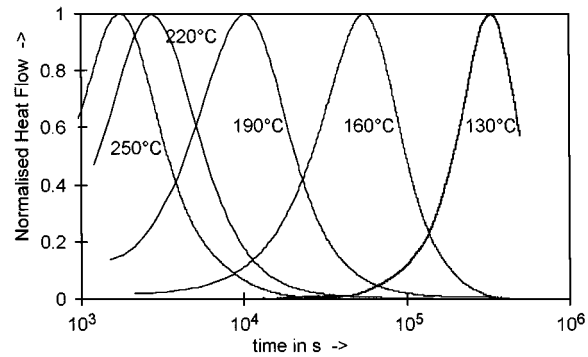

Figure 5 Normalised exothermic heat flow during isothermal ageing of the Al-16Mg alloy.

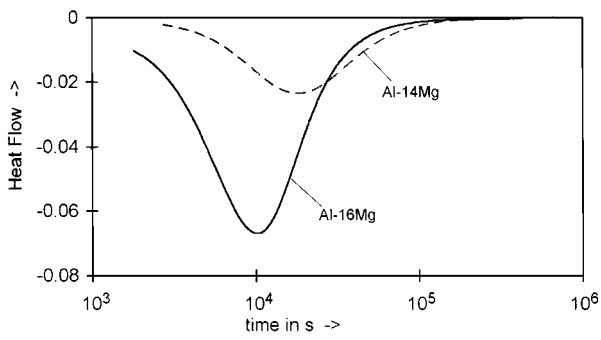

Figure 6 Heat flow during isothermal ageing at 190 °C of the furnace-cooled Al-14Mg and Al-16Mg alloys.

As a further means of verification of our interpretation of these exothermic effects observed by isothermal calorimetry, samples were aged at various temperatures and subsequently analysed by DSC. The resulting curves (Fig. 7) show three main effects D, E and F, which have been attributed to (see [14]) β' dissolution, a transformation from β' to β, and β dissolution, respectively. Hence, in correspondence with the TEM analysis, the DSC experiments show that in all these samples β' phase is present. The smaller effect G has been ascribed to (incipient) melting of the equilibrium β phase [14].

The combination of Equations 6 and 8 is used to fit the isothermal heat evolution curves. It is observed that for $T < 220$ °C all fits were close to perfect (see Fig. 8).

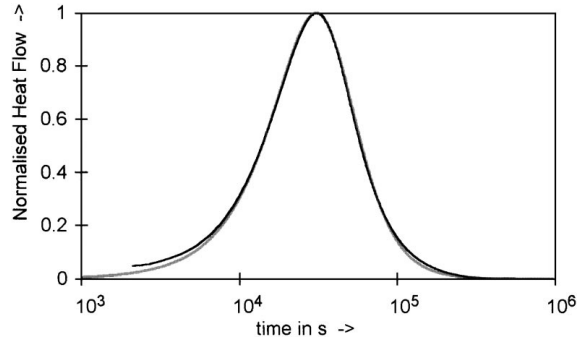

Figure 8 Normalised exothermic heat flow measured for the Al-16Mg alloy aged at 170 °C (thin, black line) compared with the fit based on Equations 6 and 8 (grey line).

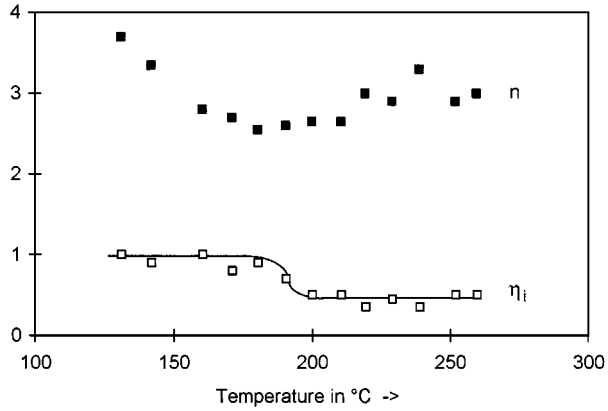

Figure 9 Parameters n and η_i as obtained from fits of the calorimetric curves for furnace-cooled Al-16Mg samples.

For $T > 220\,^{\circ}\mathrm{C}$ fits are nearly perfect up to the time that the heat flow had decreased to half the peak value, beyond this stage the fit predicted a heat flow which is slightly lower than the measured one. The values of n and η_i obtained from the fits for the furnace-cooled Al-16Mg alloy are plotted in Fig. 9. The n values of about 2.7 obtained for the furnace-cooled Al-14Mg alloy at 190 and 220 °C are similar to the ones for the furnace-cooled Al-16Mg alloy. Also the η_i values are about the same (0.35 at 220 °C). To study the effect of cooling rate on n, Al-16Mg samples were additionally cooled in air or quenched into ice-water. The values obtained from subsequent calorimetric curves during ageing at 150 °C are presented in Fig. 10. It is noted that n increases with cooling rate from 3 for furnace-cooled samples to 5 for IWQ samples.

The values for η_i resulting from the fitting with Equations 8 (see Fig. 9) are completely incompatible with the JMAK model which predicts infinitely large values for η_i. Instead, for the furnace-cooled samples the values η_i for $T < 190\,^{\circ}\mathrm{C}$ are close to unity and the AR equation gives a good approximation for the curves in this range of temperatures. The model in Section 3 predicts that for diffusion controlled growth of precipitates which grow in all directions and which nucleate at a constant rate, n should equal $2\frac{1}{2}$. From Fig. 9 it is indeed observed that for T in the range of 160–190 °C this mechanism may hold.

For $T > 200\,^{\circ}\mathrm{C}$ n increases to about 3, whilst η_i reaches a value of about 0.5 ($\lambda_i \approx 3$). This value of n is higher than the one for a transformation via random nucleation (see Section 3.1); it will be discussed in the next section and compared with the situation for $T < 160\,^{\circ}\mathrm{C}$.

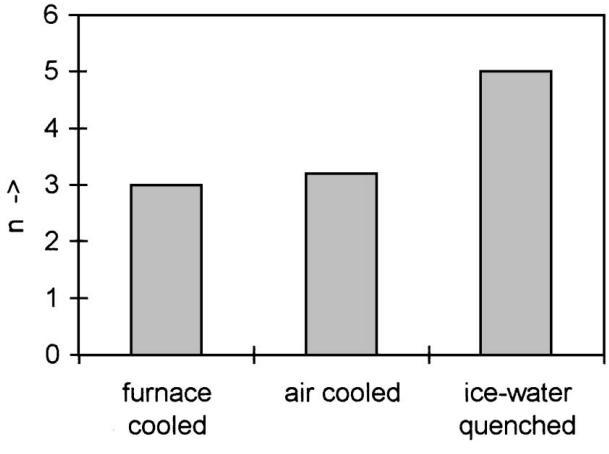

Figure 10 n values for Al-16Mg samples cooled at different rates. Ageing temperature about 150 °C.

5. Discussion

5.1. The kinetics of β' formation

From Fig. 4 it is observed that during ageing at 190 °C l_{ch} changes very little for a large part of the transformation process. It is also noted that l_{ch} increases with ageing temperature. Hence, for this transformation process, a state variable, i.e. a single variable which defines the state of the transformation for all types of isothermal or non-isothermal ageing, does not exist. Consequently, descriptions of the reaction rate by an equation of the type:

$$\frac{d\alpha}{dt} = g(T)\,f(\alpha) \qquad (10)$$

with $f(\alpha)$ a function depending only on the fraction transformed, and the rate constant, $g(T)$, a function of temperature, can not be valid for the present transformation. In addition, variation of both n and η_i with temperature shows that $f(\alpha)$ is a temperature dependent function. This is further proof that Equation 10 is invalid for the present precipitation process. As a consequence, it is not possible to perform a standard activation energy analysis on the present calorimetry data as this type of analysis assumes: (i) the validity of Equation 10 (see [29, 30]), (ii) the existence of a state variable (see [30]), and (iii) a single Arrhenius type temperature dependency of the process (see also [31]).

Between 160 and 190 °C the transformation data of β' formation in furnace cooled Al-16Mg as obtained by calorimetry is consistent with the AR equation which holds for various precipitation reactions [24]. For $T > 200\,^{\circ}\mathrm{C}$ this is no longer the case and n increases to about 3. As m for the diffusion controlled growth of the β' precipitates should still be $1\frac{1}{2}$, this value of n indicates that the nucleation rate increases as $t^{\frac{1}{2}}$ and that hence the number of nuclei increases as $t^{1\frac{1}{2}}$. For $T < 160\,^{\circ}\mathrm{C}$, n increases to reach values around $3\frac{1}{2}$. This implies that at these temperatures the nucleation rate increases with time and an n value of $3\frac{1}{2}$ would be consistent with the nucleation rate increasing linearly with t. An n value of 5 as observed for β' formation in IWQ Al-16Mg (see Fig. 10) indicates that for these samples the nucleation rate increases as $t^{2\frac{1}{2}}$.

An n value in excess of 2.5, as found for precipitation in IWQ Al-16Mg and for furnace cooled Al-16Mg alloys aged at $T < 160\,^{\circ}\mathrm{C}$ and $T > 200\,^{\circ}\mathrm{C}$, indicates that the precipitation reaction is autocatalytic, i.e. existing precipitates enhance the formation of new precipitates. Recently, β' precipitation during DSC experiments on IWQ Al-16Mg and on Al-16Mg alloys which were cooled at about 200 °C/min have been analysed using

a new method for evaluating n values for nucleation and growth reactions performed at constant heating rate [14]. In these samples β' precipitation occurs between about 210 and 300 °C for heating rates between 1.25 and 80 °C/min, and a novel analysis method of the DSC curves indicated that the transformation exponent s, which is akin to the Avrami parameter n, is well in excess of 2.5. Hence, also in these experiments autocatalytic formation of β' occurs. From a consideration of several possible mechanisms for autocatalytic nucleation it was concluded that emission of vacancies on formation of precipitates is the most likely mechanism. Specifically this means that the very first precipitates form in regions which are enriched in solute (possibly a cluster). Various researchers (see e.g. [13, 32] have in the past pointed out that due to the relaxation of misfit resulting from clustering of vacancies with Mg atoms (which is responsible for the high binding energy of vacancies with Mg atoms), Mg atoms can be expected to be situated near vacancy clusters or defects resulting from vacancy condensation (e.g. vacancy loops). Thus the formation of a precipitate from these solute clusters leads to the dissolution of the vacancy type defect. The vacancies emitted in this process can subsequently diffuse away from the newly formed precipitate and accelerate further precipitation by enhancing the diffusion of Mg atoms. It is thought that for the present calorimetry experiments at $T > 200$ °C the same mechanism operates. However, the presence of a second temperature range for autocatalytic formation ($T < 160$ °C) well separated from the other temperature range suggests that in the lower temperature range a different mechanism operates. To get more insight in this possible second mechanism, the very early stages of precipitation at low temperature will be investigated in the next section.

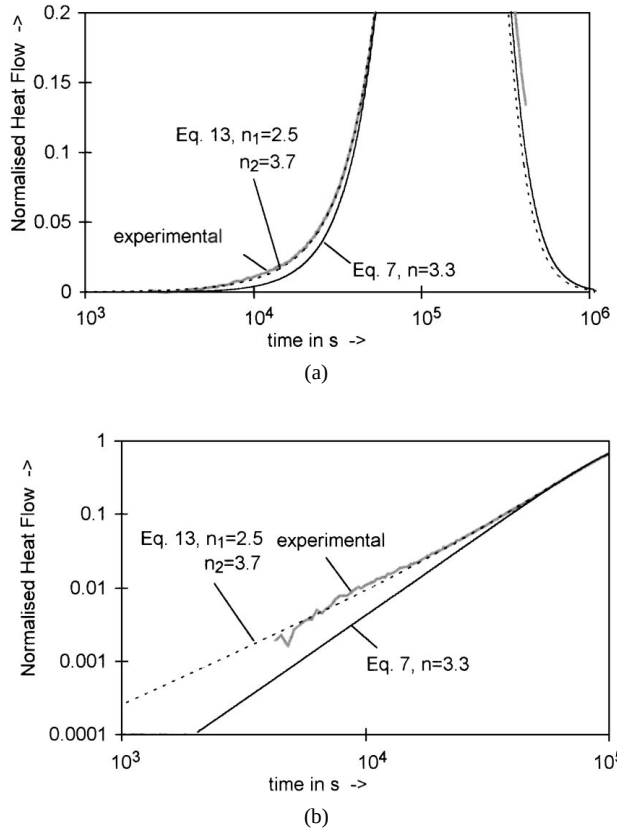

Figure 11 Normalised heat flow during ageing at 140 °C after furnace cooling (grey line). The two fits show that the initial stage of the heat effect is due to two reactions. (a: single logarithmic scale; b: double logarithmic scale).

5.2. The initial stages of the transformation

For low ageing temperatures (<160 °C), where the heat evolution during the very first stages of the β' precipitation reaction can be measured, a detailed analysis of the start of the reaction is performed. This analysis shows that up to $\alpha \approx 0.1$ the fits described above slightly underestimate the measured heat effects, indicating an initial process different from the main process. To derive an n value for this initial process we use the following expansion of the theory presented in Section 3. When a transformation resulting in a single transformation product occurs via two distinct processes (for instance grain boundary precipitation and precipitation in grains), α_{ext} is given by:

$$\alpha_{\text{ext}} = \int_0^t C_1 I_1(z)[G_1(t-z)]^{m_1}\,\mathrm{d}z + \int_0^t C_2 I_2(z)[G_2(t-z)]^{m_2}\,\mathrm{d}z \qquad (11)$$

where the symbols have the same meanings as before, whilst subscripts 1 and 2 stand for process 1 and process 2. For the case where both processes occur via either constant nucleation rate or site saturation it follows:

$$\alpha_{\text{ext}} = k_1(T)t^{n_1} + k_2(T)t^{n_2} \qquad (12)$$

The relation between α and α_{ext} is again assumed to be given by Equation 8. Equation 12 yields a nearly perfect fit with $n_1 = 2.5$ for the process that dominates the initial stage and $n_2 = 3.7$ (see Fig. 11, in which for comparison also the optimised fit, with $n = 3.3$, for a single process is given). The first process gives the largest contribution to the heat effect at the very beginning of the heat effect ($\alpha < 1 \times 10^{-6}$) whilst later on in the transformation (i.e. the overwhelming majority of the heat effect) the second process dominates. Note that as we are here studying the initial stages of the reaction ($\alpha < 0.01$), impingement is negligible and will not influence the determination of n_1.

In discussing the nature of the first process it is noted that the value of $n_1 = 2.5$ for the initial process excludes that this process involves grain boundary or grain corner nucleation, since, providing the nucleation rate does not increase, $n \leq 2$ for these processes (see [19]). As mentioned before, TEM readily shows that vacancy loops are abundantly present and one may consider that the initial process is related to the condensation of excess vacancies into loops. However, from a study of lattice parameter variations in Al-Mg alloys, van Mourik *et al.* [33] concluded that excess vacancies disappear (i.e. are

annealed out or precipitate into defects) within 1000 s at temperatures around 140 °C and this precludes that the first stage of the exothermic effect is due to clustering of vacancies.

It is thought that the very first stage of precipitation at $T \sim 140$ °C involves the nucleation of a number of precipitates which due to the fact that they are the first ones cannot be autonucleated. Hence, for this very first stage of the precipitation process, nucleation occurs at a constant rate. The obtained value for n_1 of 2.5 is consistent with this interpretation. Only in a later stage the vacancies emitted in a region around these very first precipitates will have diffused away from the precipitates and are available for further nucleation of precipitates. It is at this stage that the autocatalytic process will (gradually) gain in importance and will (gradually) take over from the first process. Hence these types of processes can fully explain why the two process model of Equation 13 fits to the experimental curve. It should, however, be noted that this correspondence between model and experiment cannot show which process is actually responsible for the emission of vacancies. One may consider the mentioned dissolution of vacancy type defects (mainly loops), but also vacancies bound to Mg atoms will be released on precipitation of the companion Mg atom. Hence, two possible mechanisms may be identified, and it is suggested that these two mechanisms are responsible for the two ranges of autocatalytic nucleation observed in this study.

Finally it is noted that the discussion presented in this section illustrates the extraordinarily high accuracy that can be obtained by the Tian-Calvet isothermal calorimeter. The calorimetry experiments show clearly that at low temperatures (<160 °C), before the main (autocatalytic) precipitation reaction starts, an initial process with a lower n value occurs. Any attempt at detection of β' phase (or possible precursors) at these extremely low fractions transformed by other types of experiments (for instance TEM) will be either extremely time consuming or outright impossible.

6. Conclusions

Isothermal β' precipitation in Al-13 at % Mg and Al-16 at % Mg has been studied by isothermal calorimetry, transmission electron microscopy (TEM), optical microscopy and differential scanning calorimetry (DSC). The following conclusions are drawn:

- The isothermal calorimetry curves can be fitted over the entire range of transformation by a recently developed variant of the Johnson-Mehl-Avrami-Kolmogorov (JMAK) model and the characteristic reaction exponent n is derived.
- For Al-Mg n increases with quenching rate.
- For furnace cooled Al-16Mg aged at $T < 160$ °C and $T > 200$ °C, n is larger than 2.5, indicating an autocatalytic precipitation process. The mechanisms for this autocatalytic process are discussed, and evidence is presented pointing at emission of vacancies on the formation of nuclei as being the essential step in the autocatalytic process.
- A detailed analysis of the very first stage of the calorimetry curves of furnace cooled Al-16Mg during ageing at 140 °C reveals that β' precipitation is a two stage process, with the first stage being nucleation at constant rate ($n_1 = 2.5$) and the second stage being autocatalytic nucleation ($n_2 > 2.5$).
- For β' precipitation the commonly used equation:

$$\frac{d\alpha}{dt} = g(T)\, f(\alpha)$$

is not valid. This follows from (a) the strong variation of the characteristic length of the β' precipitates with ageing temperature, which indicates that the definition of a state variable is not possible, and (b) the variation of function $f(\alpha)$ with temperature.

Acknowledgements

This work is financed in part by the EC Human Capital and Mobility project. The authors are grateful to C. Zahra for technical assistance and to Dr. A. Charaï of CP2M, Université d'Aix-Marseille III, and Mr. S. Nitsche of CRMC2 du CNRS, Marseille, for making available TEM facilities. Prof. J.-P. Crousier is thanked for making available optical microscopy facilities.

References

1. K. OSAMURA and T. OGURA, *Metall. Trans.* **15A** (1984) 835.
2. A. DAUGER, E. K. BOUDILI and M. ROTH, *Scripta. Metall.* **10** (1976) 1119.
3. R. NOZATO and S. ISHIHARA, *Trans. Japan. Inst.* **21** (1980) 580.
4. M. BERNOLE, PhD thesis, University of Rouen, Rouen, 1974.
5. M. BOUCHEAR, D. HAMANA and T. LAOUI, *Phil. Mag A.* **73** (1996) 1733.
6. A. DAUGER, M. FUMERON, J. P. GUILLOT and M. ROTH, *J. Appl. Cryst.* **12** (1979) 429.
7. T. SATO, Y. KOJIMA and T. TAKAHASHI, *Metall. Trans.* **13A** (1982) 1373.
8. M. BERNOLE, J. RAYNAL and R. GRAF, *J. de Microscopie* **8** (1969) 831.
9. S. NEBTI, D. HAMANA and G. CIZERON, *Acta Metall. Mater.* **43** (1995) 3583.
10. P. van MOURIK, N. M. MAASWINKEL, TH. H. de KEIJSER and E. J. MITTEMEIJER, *J. Mater. Sci.* **24** (1989) 3779.
11. J. D. EMBURY and R. B. NICHOLSON, *Acta Metall.* **11** (1963) 347.
12. G. ITOH, B. COTTEREAU and M. KANNO, *Mater. Trans. JIM* **31** (1990) 1041.
13. A. EIKUM and G. THOMAS, *Acta Metall.* **12** (1964) 537.
14. M. J. STARINK and A.-M. ZAHRA, *Acta Mater.* **46** (1998) 3381.
15. C. Y. ZAHRA and A.-M. ZAHRA, *Thermochim. Acta* **276** (1996) 161.
16. M. J. STARINK and A.-M. ZAHRA, *ibid.* **292** (1997) 159.
17. *Idem., Phil. Mag. A* **77** (1998) 187.
18. F. L. CUMBRERA and F. SANCHEZ-BAJO, *Thermochim. Acta* **266** (1995) 315.
19. J. W. CHRISTIAN, "The Theory of Transformation in Metals and Alloys," 2nd ed., Part 1 (Pergamon Press, Oxford, UK, 1975).
20. M. AVRAMI, *J. Chem. Phys.* **7** (1939) 1103.
21. *Idem., ibid.* **8** (1940) 212.
22. *Idem., ibid.* **9** (1941) 177.
23. V. SESSA, M. FANFONI and M. TOMELLINI, *Phys. Rev. B* **54** (1996) 836.
24. M. J. STARINK, *J. Mater. Sci.* **32** (1997) 4061.

25. EON-SIK LEE and YOUNG G. KIM, *Acta Metall. Mater*. **38** (1990) 1669.
26. M. J. STARINK and A.-M. ZAHRA, *Phil. Mag*. **76** (1997) 701.
27. D. HAMANA, S. NEBTI, A. BOUTEFNOUCHET and S. CHEKROUD, *Z. Metallkd*. **84** (1993) 33.
28. D. HAMANA, S. NEBTI and M. BOUCHEAR, *ibid*. **87** (1996) 135.
29. M. J. STARINK, *J. Mater. Sci*. **32** (1997) 6505.
30. E. J. MITTEMEIJER, *J. Mater. Sci*. **27** (1992) 3977.
31. M. J. STARINK and A.-M. ZAHRA, Proc. of ICAA-5, Grenoble, France, *Mater. Sci. Forum* **217–222** (1996) 795.
32. R. E. SMALLMAN and A. EIKUM, in Proc. of Lattice Defects in Quenched Materials, Argonne, Illinois, USA, June 1964, edited by R. M. J. Cotterill, M. Doyama, J. J. Jackson and M. Meshii (Academic Press Inc., London, 1965) p. 591.
33. P. van MOURIK, TH. H. de KEIJSER and E. J. MITTEMEIJER, in Proc. of the 5th International Conf. on Rapidly Quenched Materials, edited by S. Steeb and H. Warlimont (North Holland, Amsterdam, 1985) p. 899.

Received 3 December 1996
and accepted 13 October 1998